CPUE standardization for swordfish (*Xiphias gladius*) by Japanese longline fishery in the Indian Ocean using zero-inflated Bayesian hierarchical spatial model

Takayuki Matsumoto[1]*, Kenji Taki[1], Hirotaka Ijima[1], and Mikihiko Kai[1]
*matsumoto_takayuki77@fra.go.jp

[1] *Fisheries Resources Institute, Japan Fisheries Research and Education Agency, 2-12-4, Fukuura, Kanazawa-ku, Yokohama-shi, 236-8648, Japan*

Summary

Standardization of swordfish CPUEs (1979-1993, 1994-2022) in the Indian Ocean by Japanese longliners was conducted for the datasets in four areas (NW, NE, SW, SE). We applied Bayesian hierarchical spatial models. Since the catch data include many zeros, we evaluated zero-inflated Poisson GLMM (ZIP-GLMM). Best candidate model was selected based on Widely Applicable Bayesian Information Criterion (WAIC). From the lowest value of WAIC, spatial Poisson GLMM with autoregressive (AR1) modelled for the year trend (i.e. m_zip_spde2 model) was selected as the best candidate for each area except for SE area. The trends of CPUEs were generally similar among areas with slight differences.

1. Introduction

Hierarchical Bayesian models have traditionally relied on Markov chain Monte Carlo (MCMC) simulation techniques, which are computationally expensive and technically challenging, consequently limiting their use. However, a new statistical approach is currently readily available, namely integrated nested Laplace approximations (INLA) via the R-INLA package (http://www.r-inla.org). INLA methodology and its powerful application to modelling complex datasets has recently been introduced to wider nontechnical audience (Illian et al. 2013). As opposed to MCMC simulations, INLA uses an approximation for inference and hence avoids the intense computational demands, convergence, and mixing problems sometimes encountered by MCMC algorithms (Rue and Martino 2007). Moreover, included in R-INLA, the stochastic partial differential equations (SPDE) approach (Lindgren et al. 2011) is another statistical development that models spatial random effect (Gaussian random field, GRFs) much faster as well as constructs flexible fields that are better adept to handle datasets with complex partial structure (Lindgren 2013). This is often the case with fisheries data, since fishermen frequently tend to change fishing grounds, resulting in clustered spatial patterns and large regions without any values. Together, these new statistical methods and their implementation in R allows scientists to fit considerably faster and more reliably complex spatiotemporal model (Rue et al. 2009, Cosandey-Godin et al. 2015).

The aim of this paper is to grasp the historical trajectory of swordfish (*Xiphias gladius*) abundance

index in the Indian Ocean caught by Japanese longliners during 1979-2022 for the four areas (Northwest, Northeast, Southwest, and Southeast) used in the last stock assessment, applying zero-inflated Bayesian hierarchical spatial models fitted using these two techniques.

2. Materials and methods

Data sets

Japanese longline logbook data (set by set data) was used for the CPUE standardization of the swordfish in the Indian Ocean. We used the data from 1979 onwards because the number of hooks between floats and the vessel name, which commonly affect the CPUE standardization, are completely available since then. The format of the Japanese logbook was changed in 1994 and the fishing methods (e.g. materials of main and branch lines and gear configuration such as number of hooks between floats) related to catchability: q, which is not detailed in the logbook, was changed during the mid-1990s. Therefore, we divided the time-period into two, 1979-1993 and 1994-2022 for the analysis. The spatial and temporal resolution of the logbook is 1x1 grid scale and day, respectively. We used the same four analysis areas (NW, NE, SW, and SE) of Indian Ocean set in the 9th session of the IOTC working party on billfish for the standardization analysis of Swordfish (IOTC 2014; **Fig. 1**).

Statistical models

In this analysis, we applied Bayesian hierarchical spatial models. We did not apply the spatiotemporal models because the spatiotemporal model is computationally expensive and the values of Widely Applicable Bayesian Information Criterion (WAIC; Watanabe, 2013) did not differ so much between spatial and spatiotemporal models in the past analysis (Taki et al., 2020). Since the catch data include many zeros (**Fig. 2**), we evaluated zero-inflated Poisson GLMM (ZIP-GLMM). The zero-inflated model is useful because this model can estimate "true" zero catch. To apply zero-inflated negative binomial GLMM (ZINB-GLMM) is another way to consider the many zero issue, but the ZINB tends to cause underdispersion (e.g., Ijima 2017), thus we think zero-inflated Poisson GLMM (ZIP-GLMM) is more appropriate to use for the CPUE standardization.

For the explanatory variables, year (yr) and quarter (Jan-Mar, Apr-Jun, Jul-Sep, Oct-Dec; qtr) were given as fixed effect, and area (latlon), gear configuration; number of hooks between floats (hpb), and fleet (jp_name) were given as random effect. The hpb generally increased to the mid-1990s (**Fig. 3**). Most variables were treated as categorical variables but the autoregressive model (AR1) was applied to years for some spatial models in considering the large uncertainties. Including the random effect in the model is appropriate because these effects such as the vessel name (jp_name), gear configuration (hpb), and 5x5 area (latlon) have a lot of variables. The random effect model can also remove the pseudo-replication by vessel, gear configuration and operating area.

All analyses were performed using R, specifically the R-INLA package. The INLA procedure, in

accordance with the Bayesian approach, calculates the marginal posterior distribution of all random effects and parameters involved in the model. We applied half Cauchy distribution as a prior for the random effect. Best candidate models were selected based on Widely Applicable Bayesian Information Criterion (WAIC).

3. Results and discussions

3.1. Overview of catch and effort

Distribution of fishing effort by Japanese longline fishery is shown in **Fig. 4** (entire period), **Fig. 5** (by decade) and **Fig. 6** (annually from 1996). Fishing effort is distributed in the almost entire Indian Ocean, but there is few or no fishing effort in the central south area. Distribution of fishing effort is more sparse in recent years (after 2010s). From late 2000s, fishing effort in the southeast area is concentrated in the eastern part (west off Australia) due to the reduction of total fishing efforts.

Fig. 7 shows distribution of species composition of the longline catch by decade. In the tropical area, bigeye and/or yellowfin tuna were dominant, whereas southern bluefin and/or albacore were dominant in the temperate area. Swordfish was usually not a main component of the catch in each area. This result means that the Japanese longline fishery has not targeted the swordfish in the Indian Ocean.

Fig. 8 shows distribution of nominal CPUE (number of fish per 1000 hooks) of swordfish by Japanese longline fishery in the Indian Ocean (average for 1979-2022). Generally, CPUE is higher in the tropical area especially in the western part. In addition, higher CPUE is observed in the southeast area (west and south off Australia).

Fig. 9 shows mean body weight (kg) of swordfish caught by Japanese longline fishery in the Indian Ocean (average for 1979-2022). Mean body weight was higher in the temperate area than in the tropical area. In the temperate (south) area between 30S and 40S, mean body weight was higher in the western part (west of 80 E) than in the eastern part (east of 80 E).

3.2. Standardized CPUE

We examined the total of eight models (4 areas, 2 periods). From the lowest value of WAIC, spatial Poisson GLMM with autoregressive (AR1) modelled for the year trend (i.e. m_zip_spde2 model) was selected as the best candidate for each area except for SE area (**Table 1**).

Northwest

The posterior probability distribution is shown in **Fig.** 10, and the estimated marginal distributions seems reasonable. The mean of latent spatial field indicated that the southeastern part has been negatively affected for the standardized CPUE during 1994-2022, while the western coastal part has been positively affected for the standardized CPUE throughout the period (**Fig.** 11). No apparent trend in interannual variation of standardized CPUE was observed (**Fig.** 12, Table 2).

Northeast

The posterior probability distribution is shown in **Fig. 13**. The western offshore part (south of India) has been positively correlated with the swordfish CPUE throughout the period (**Fig. 14**). No apparent trend in interannual variation of standardized CPUE was observed (**Fig. 15**, Table 3).

Southwest

The posterior probability distribution is shown in **Fig. 16**. The western coastal part has been positively correlated with the swordfish CPUE throughout the period (**Fig. 17**). No apparent trend in interannual variation of standardized CPUE was observed (**Fig. 18**, Table 4).

Southeast

From the WAIC, spatial and non-zero-inflated model (m_spde2) was selected during 1979-1993, while non- spatial and zero-inflated model (m_zip_glmm) was selected during 1994-2022. The posterior probability distribution is shown in **Fig. 19**. Southern part has been negatively correlated with the Swordfish CPUE during 1979-1993 (**Fig. 20**). No apparent trend in interannual variation of standardized CPUE was generally observed for each area (**Fig. 21**, Table 5).

Fig. 22 shows comparison of relative CPUE among areas. Overall trend is similar among areas, but there are some differences. For example, CPUE sharply declined during late 1980s to early 1990s in the southwest area, whereas the trend was comparatively stable in other areas. Decrease in CPUE was observed during mid 1990s to early 2000s for all areas, and after that increasing trend is observed except for southwest area.

Comparison with CPUE in the previous study and nominal CPUE

Fig. 23 shows the comparison with relative standardized CPUE (from 1994) with CPUE in the previous study (Taki et al., 2020), which used the same method as that in the present study, and comparison with nominal CPUE. Comparison for CPUE before 1994 is not shown because there is no change in the indices from the previous study. The trend of point estimates for standardized CPUE is similar for each area between the two studies. The trend of standardized CPUE is similar to that of nominal CPUE except for southeast area, in which the trend of nominal CPUE largely changed (got

much higher) around early 2010. Possible cause is as follows. In the southwest area, the distribution of Japanese longline operation was in a wide range except for western part before 2010 (**Fig. 6**). However, after that it became concentrated in the eastern part (west off Australia) where nominal CPUE is higher (**Fig. 8**). This may have affected the trend of nominal CPUE.

4. References

Cosandey-Godin, A., Krainski, E. T., Worm, B. and Flemming, J. M. 2015. Applying Bayesian spatiotemporal models to fisheries bycatch in the Canadian Arctic. Can. J. Fish. Aquat. Sci. 72: 186–197. dx.doi.org/10.1139/cjfas-2014-0159.

Ijima, H. 2017. CPUE standardization of the Indian Ocean swordfish (*Xiphias gladius*) by Japanese longline fisheries: Using negative binomial GLMM and zero inflated negative binomial GLMM to consider vessel effect. IOTC-2017-WPB15-19.

Illian, J.B., Martino, S., Sørbye, S.H., Gallego-Fernández, J.B., Zunzunegui, M., Paz Esquivias, M., and Travis, J.M.J. 2013. Fitting complex ecological point process models with integrated nested Laplace approximation. Methods Ecol. Evol. 4(4): 305–315. doi:10.1111/2041-210x.12017.

IOTC. 2014. Report of the 12th session of the IOTC working party on billfish. IOTC-2014-WPB-R [E].

Lindgren, F., and Rue, H. 2013. Bayesian spatial and spatio-temporal modelling with R-INLA. Journal of Statistical Software. [In press.] Rue, H., and Martino, S. 2007. Approximate Bayesian inference for hierarchical Gaussian Markov random field models. J. Stat. Plann. Infer. 137(10): 3177–3192. doi:10.1016/j.jspi.2006.07.016.

Lindgren, F., Rue, H., and Lindström, J. 2011. An explicit link between Gaussian fields and Gaussian Markov random fields: the stochastic partial differential equation approach. J. R. Stat. Soc. Ser. B Stat. Methodol. 73(4): 423–498. doi:10.1111/j.1467-9868.2011.00777.x.

Rue, H., and Martino, S. 2007. Approximate Bayesian inference for hierarchical Gaussian Markov random field models. J. Stat. Plann. Infer. 137(10): 3177–3192. doi:10.1016/j.jspi.2006.07.016.

Rue, H., Martino, S., and Chopin, N. 2009. Approximate Bayesian inference for latent Gaussian models by using integrated nested Laplace approximations. J. R. Stat. Soc. Ser. B Stat. Methodol. 71(2): 319–392. doi:10.1111/j.1467-9868. 2008.00700.x.

Taki, K., Ijima, H. and Y. Semba. 2020. Japanese Longline CPUE Standardization (1979-2018) for Swordfish (*Xiphias gladius*) in the Indian Ocean using zero-inflated Bayesian hierarchical spatial model. IOTC-2020-WPEB18-14.

Watanabe, S. 2013. A widely applicable Bayesian information criterion. Journal of Machine Learning

Research 14: 867-897.

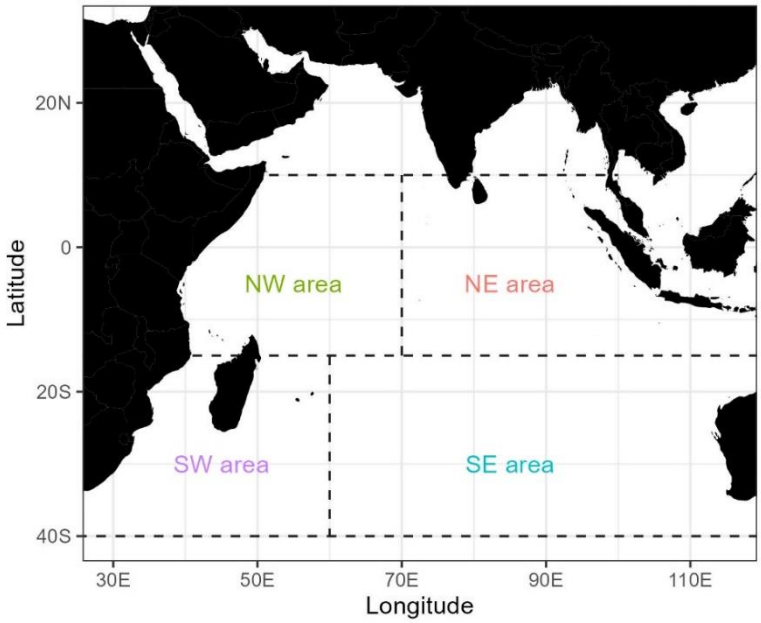

Fig. 1. Four analysis areas used for the Swordfish CPUE standardization in the Indian Ocean.

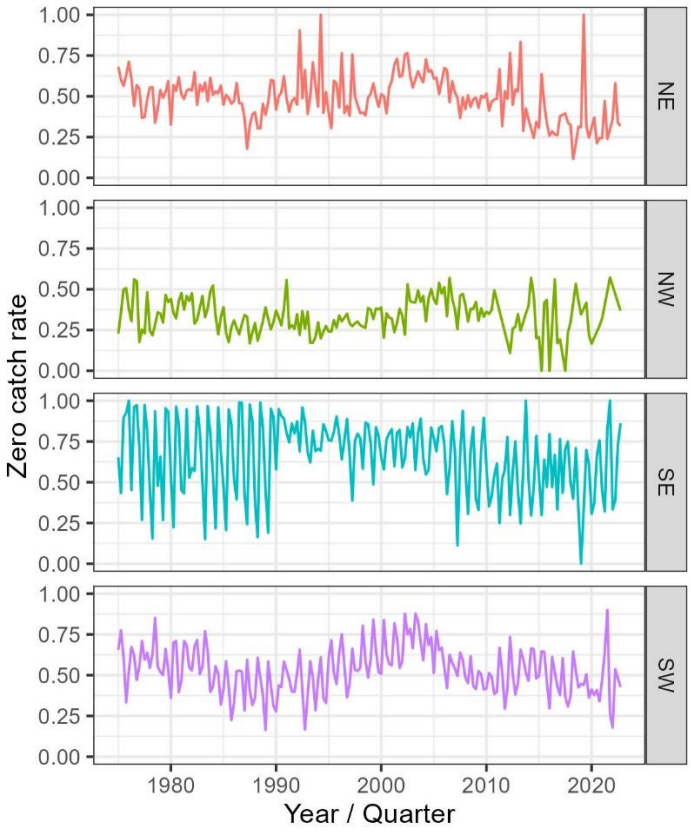

Fig. 2. Zero catch rate of swordfish caught by Japanese long line fishery in each area.

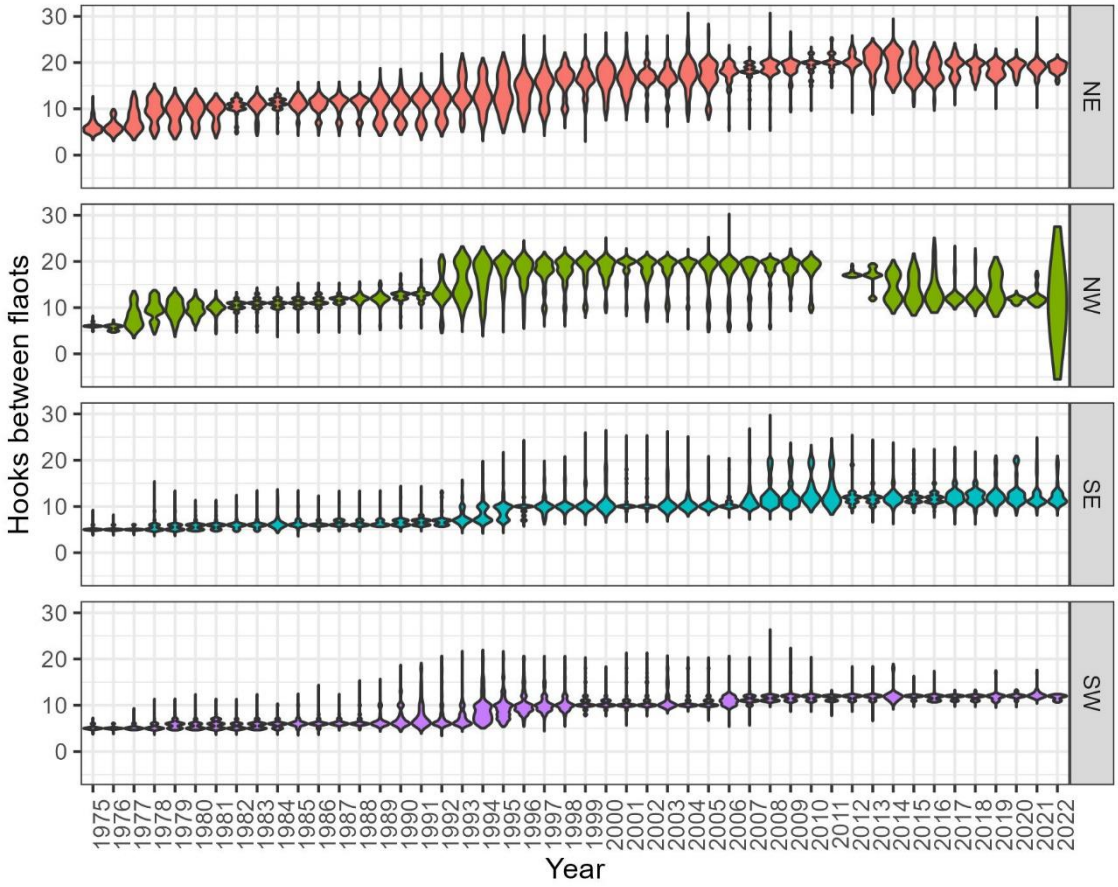

Fig. 3. Historical change in the gear setting (hooks between floats) of Japanese longline fishery in the Indian Ocean. Gear configuration is different between North and South Indian Ocean because Japanese longliners commonly targets Southern Bluefin tuna in the South Indian Ocean. Vertical range of the plots shows the range of the data, and width shows frequency of the data.

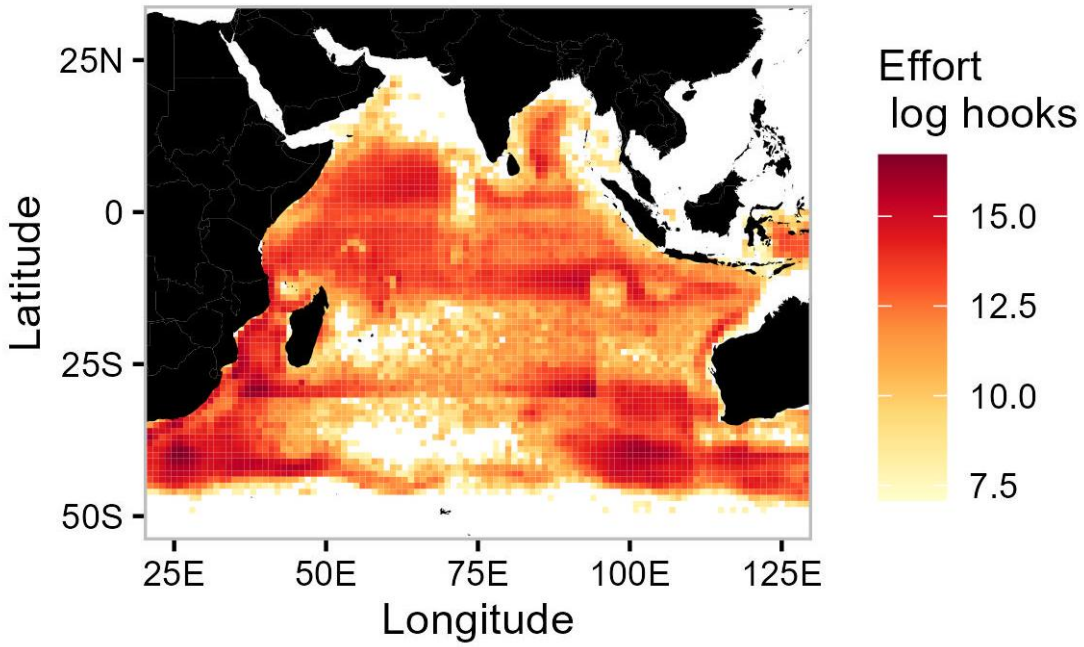

Fig. 4. Distribution of fishing effort (log of number of hooks) by Japanese longline fishery in the Indian Ocean (1979-2022).

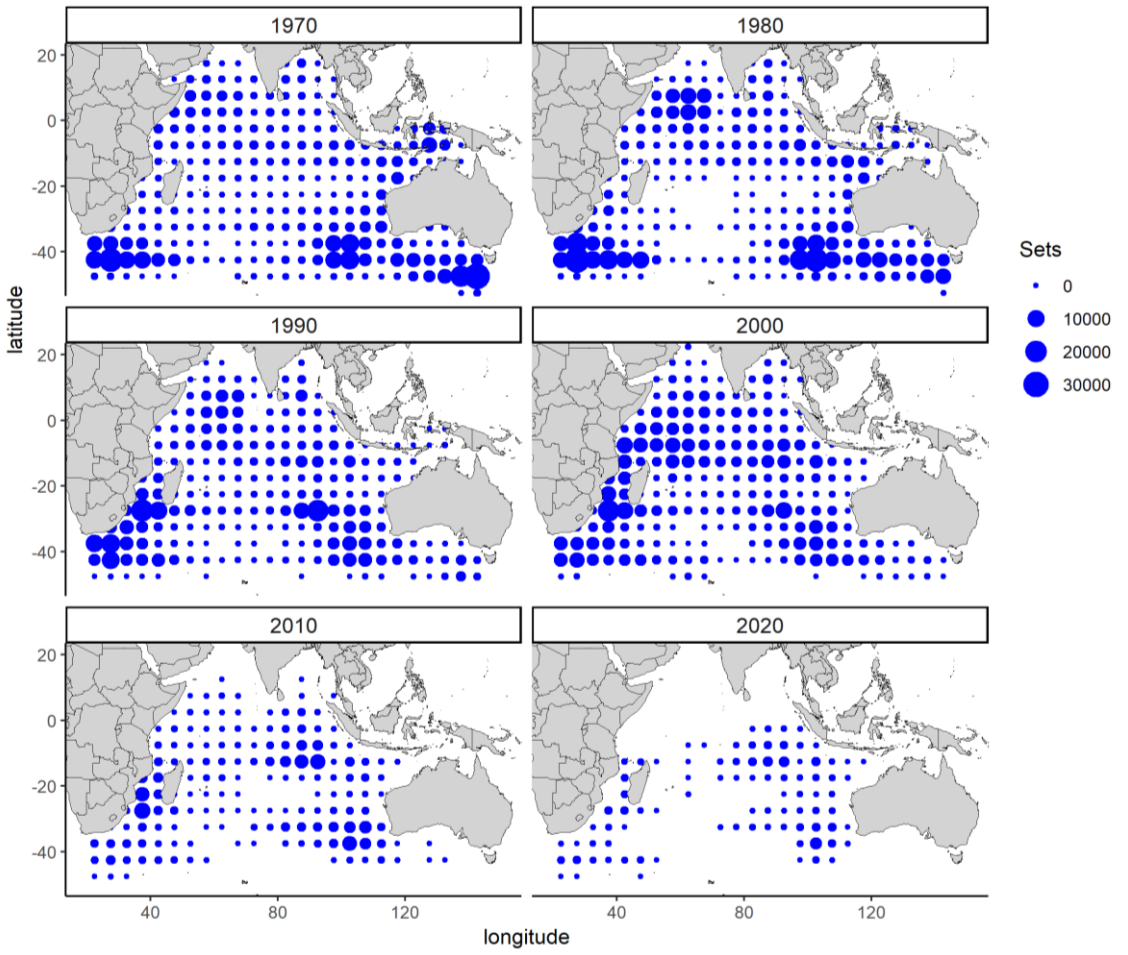

Fig. 5. Distribution of fishing effort (number of sets) by Japanese longline fishery in the Indian Ocean (by decade).

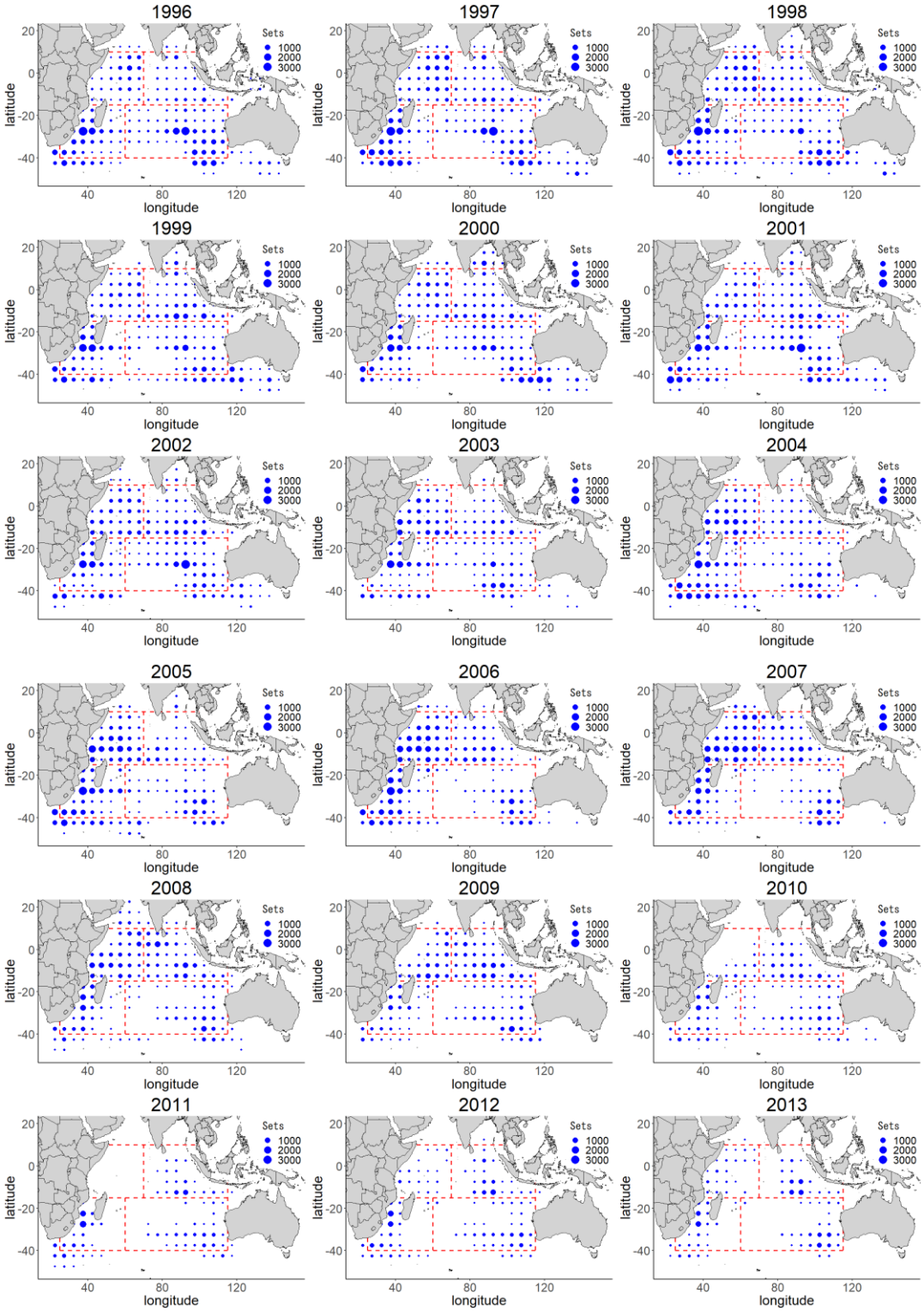

Fig. 6. Distribution of fishing effort (number of sets) by Japanese longline fishery in the Indian Ocean (annual from 1996). Dashed lines show boundary for the areas for CPUE standardization.

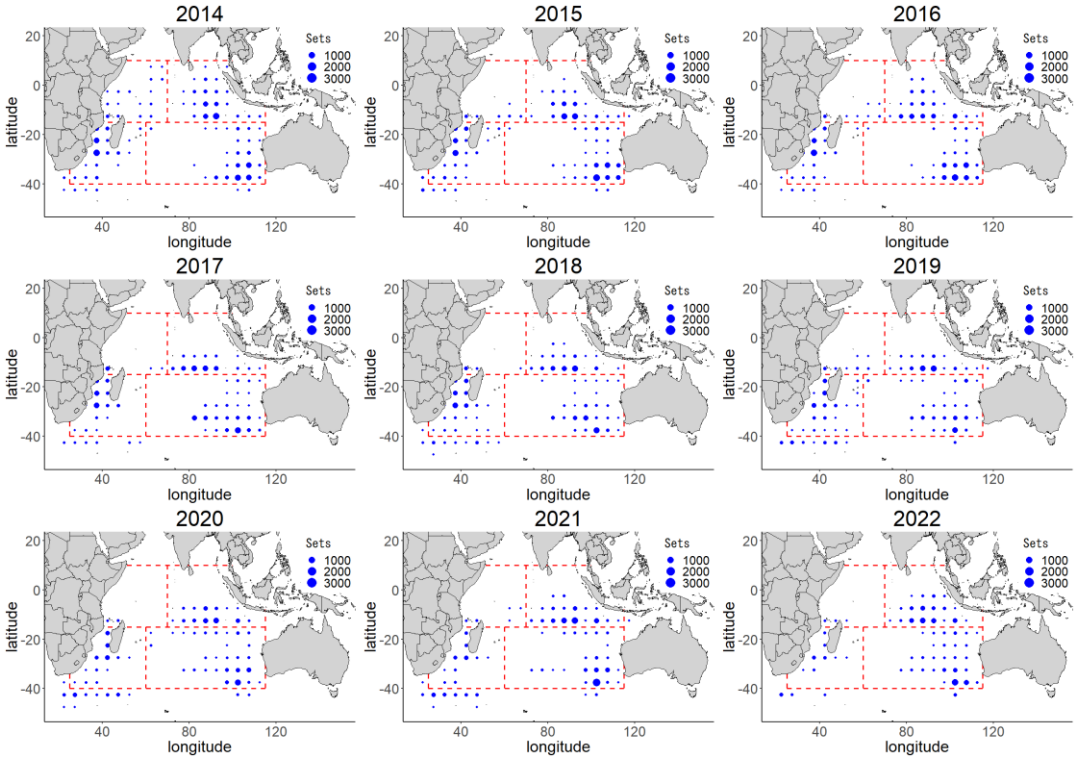

Fig. 6. Distribution of fishing effort (number of sets) by Japanese longline fishery in the Indian Ocean (annual from 1996). (continued)

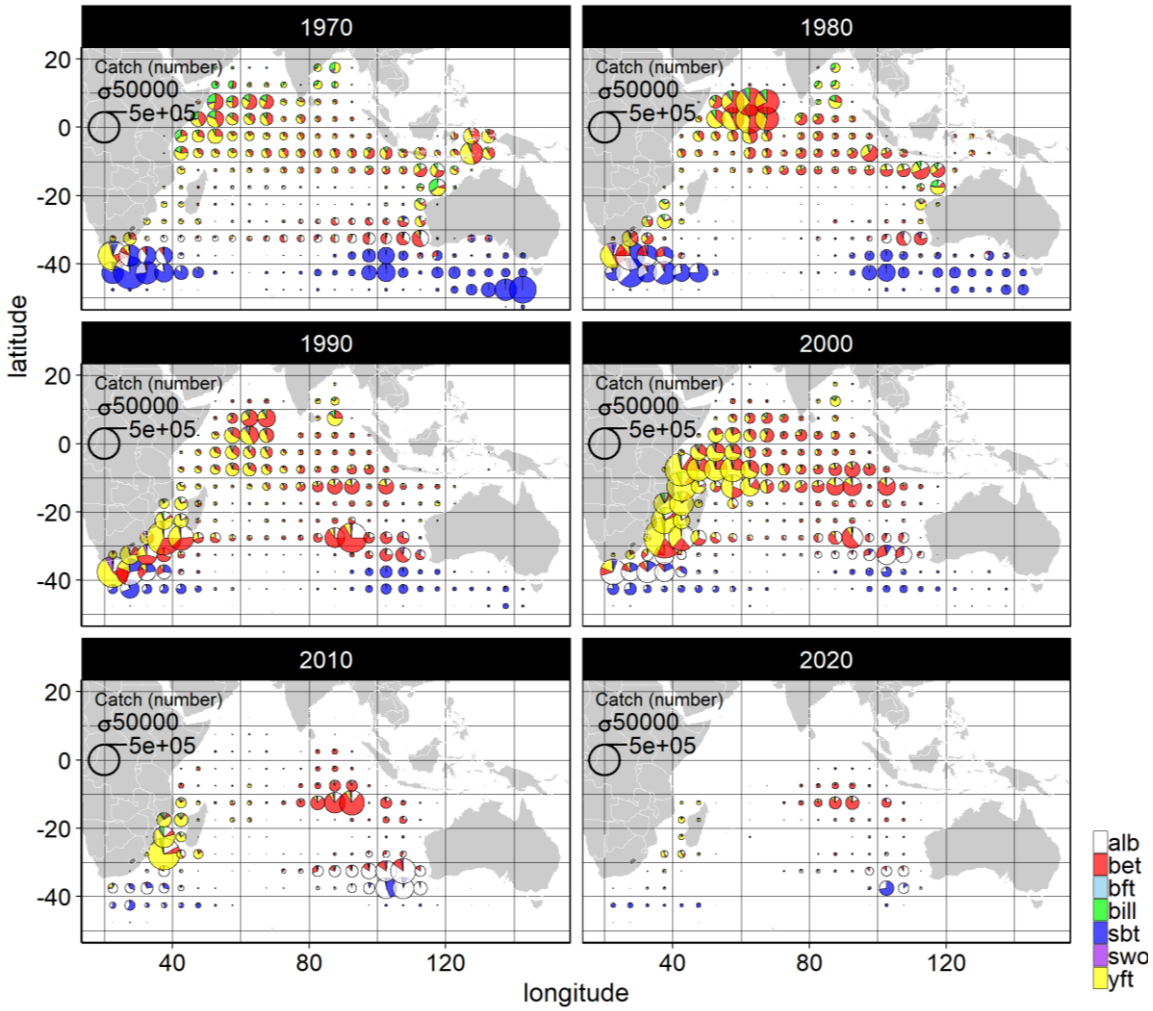

Fig. 7. Distribution of species composition of the catch in number by Japanese longline fishery in the Indian Ocean in each decade.

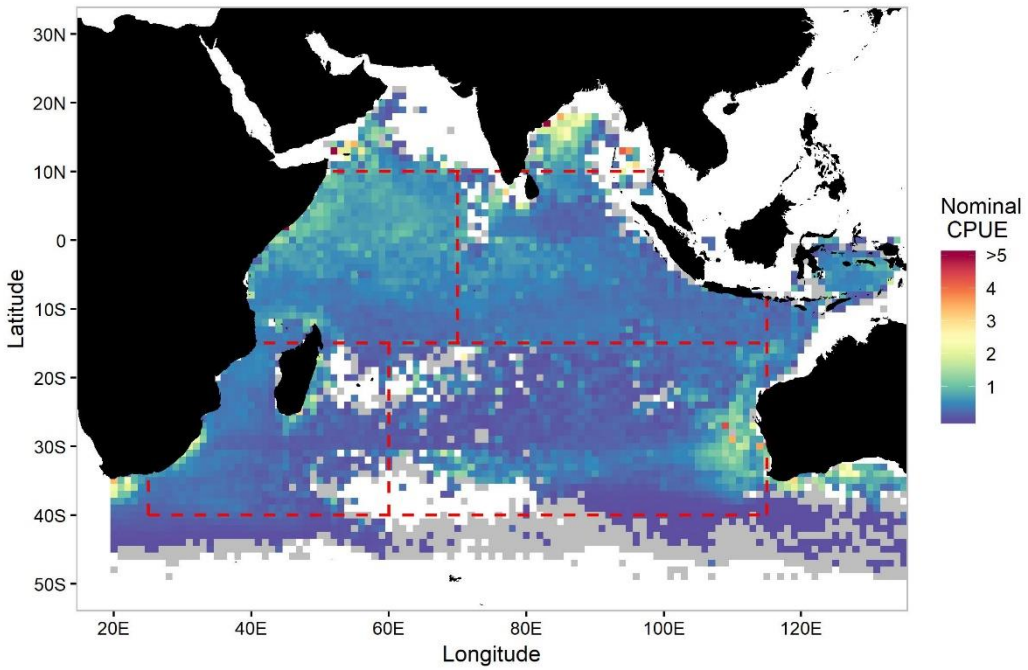

Fig. 8. Distribution of nominal CPUE (number of fish per 1000 hooks) of swordfish by Japanese longline fishery in the Indian Ocean (average for 1979-2022). Dashed lines show boundary for the areas for CPUE standardization.

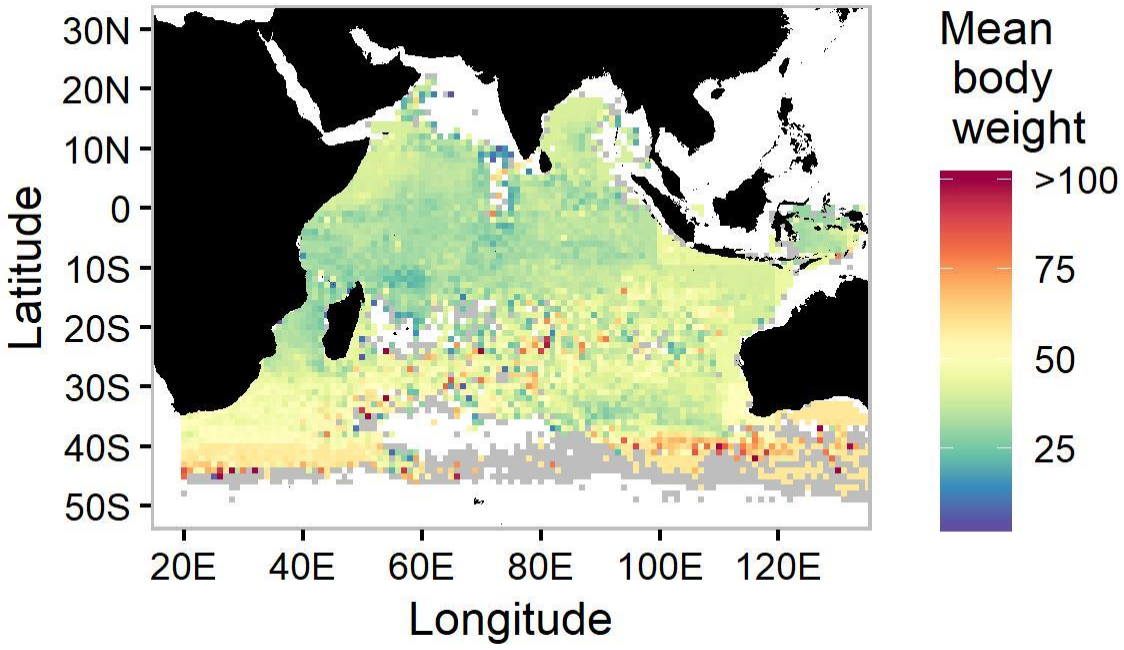

Fig. 9. Distribution of mean body weight (kg) of swordfish caught by Japanese longline fishery in the Indian Ocean (average for 1979-2022).

Table 1. Eight models and their WAIC values for two time periods of four areas. Selected models corresponded to those with the smallest values yellow-highlighted.

	NW(1979-1993)	NW(1994-2022)	NE(1979-1993)	NE(1994-2022)	SW(1979-1993)	SW(1994-2022)	SE(1979-1993)	SE(1994-2022)
m_null = inla (swo~1, data=d,offset=log(d$hooks/1000),family="poisson")	165589	345795	68131	176980	320465	345795	134496	327824
m_glm = inla (swo~yr + latlon, data=d,offset=log(d$hooks/1000),family="poisson")	154089	288654	$>10^{18}$	$>10^{18}$	$>10^{18}$	288654	$>10^{16}$	$>10^{18}$
m_glmm = inla (swo~yr + qtr + f(latlon,model="iid",hyper=hcprior) + (jp_name,model="iid")+f(hpb,model="iid"), data=d,offset=log(d$hooks/1000),family="poisson")	140089	258392	59084	144744	191961	258392	46025	194975
m_zip_glmm = inla (swo~yr + qtr + f(latlon,model="iid") + f(jp_name,model="iid"), data=d, offset=log(d$hooks/1000),family="zeroinflatedpoisson1")	137367	244205	57837	141241	183257	244205	43373	165323
m_spde = inla (swo~0 + intercept + yr + qtr + f(hpb,model="iid") + f(jp_name,model="iid") + f(w,model=spde), data=inla.stack.data(StackFit), offset=log(d$hooks/1000),family="poisson")	138833	245231	58380	143678	178481	245231	44402	180766
m_spde2 = inla (swo~0 + intercept + f(yr,model="ar1") + f(month,model="iid",hyper=hcprior) + f(hpb,model="iid",hyper=hcprior) + f(jp_name,model="iid",hyper=hcprior) + f(w,model=spde), data=inla.stack.data(StackFit2), offset=log(d$hooks/1000),family="poisson")	138155	244593	58302	143193	176021	244593	43013	173620
m_zip_spde = inla (swo~0 + intercept + yr + qtr + f(hpb,model="iid") +f(jp_name,model="iid") + f(w,model=spde), data=inla.stack.data(StackFit), offset=log(d$hooks/1000),family="zeroinflatedpoisson1")	135626	231706	57164	140008	168193	231706	52478	173903
m_zip_spde2 = inla (swo~0 + intercept + f(yr,model="ar1") + f(month,model="iid",hyper=hcprior) + f(hpb,model="iid") + f(jp_name,model="iid") + f(w,model=spde), data=inla.stack.data(StackFit2), offset=log(d$hooks/1000),family="zeroinflatedpoisson1")	135008	231288	57109	139493	166239	231288	—	—

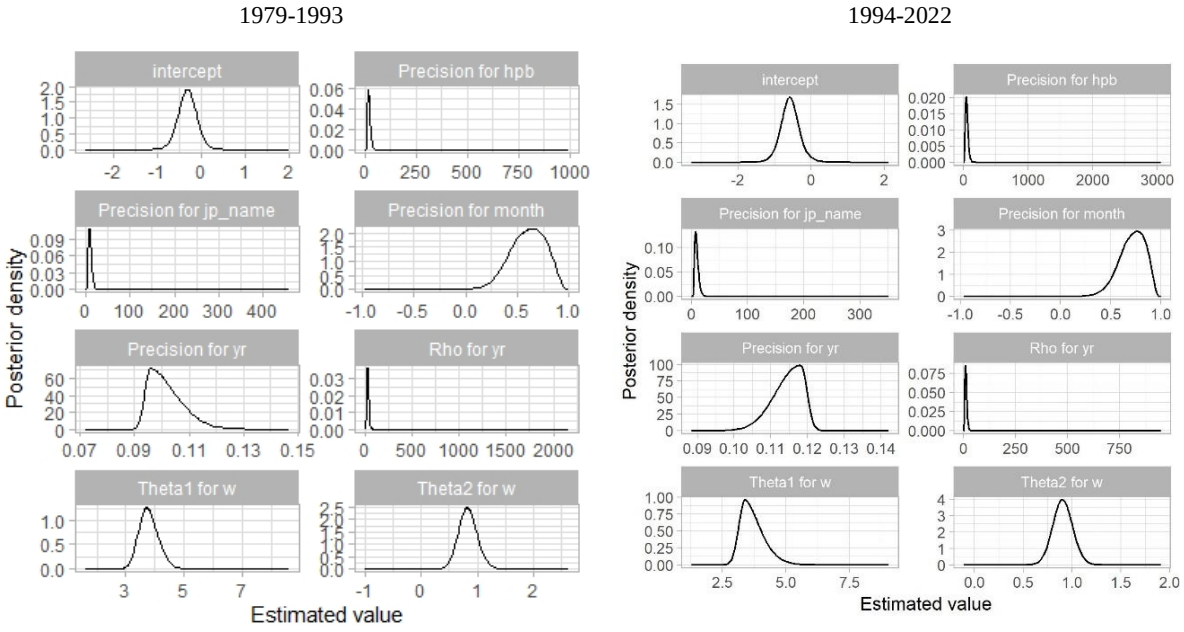

Fig. 10. Northwest. Posterior marginal distribution of the fixed effect (intercept), precision for random effects, temporal correlation term (Rho), and spatial field parameters (Thetas).

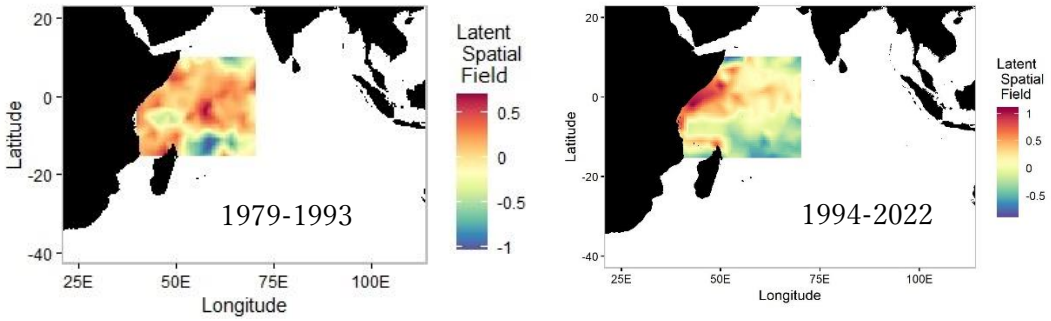

Fig. 11. Northwest. Mean of latent spatial field.

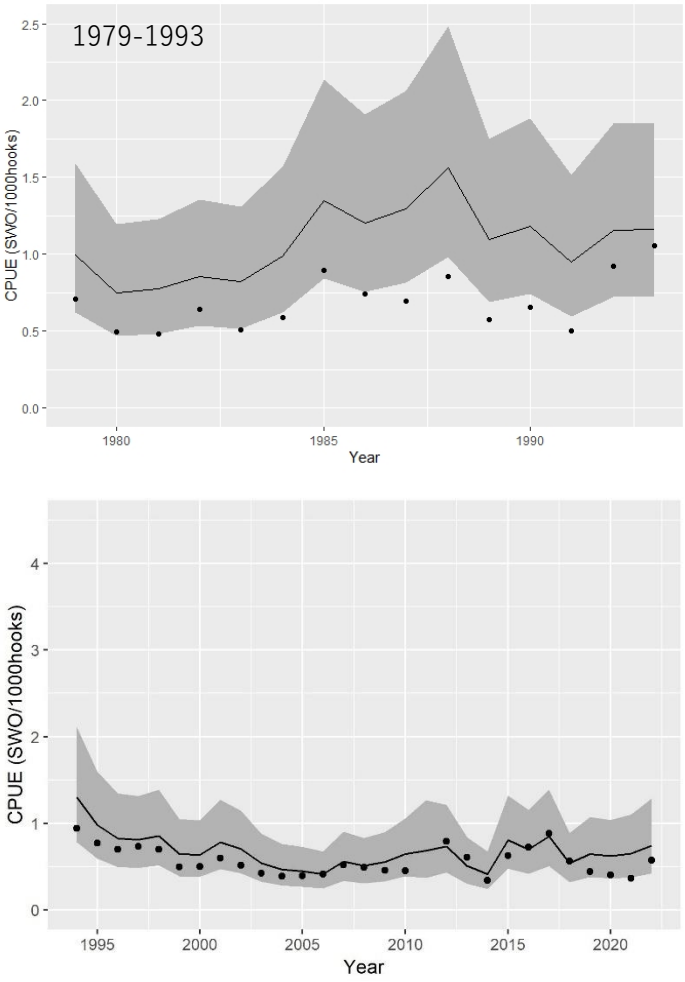

Fig. 12. Northwest. Historical changes of CPUEs. Line is standardized CPUE (number of SWO/1000 hooks) and filled area is 95% credible interval. Points denote nominal CPUE (number of SWO/1000 hooks).

Table 2. **Northwest.** Nominal and standardized CPUEs for periods 1979-93 and 1994-2022.

year	nominal	Standardized	2.50%	97.50%	year	nominal	Standardized	2.50%	97.50%
1979	0.71	1.00	0.62	1.59	1994	0.94	1.30	0.78	2.11
1980	0.50	0.75	0.47	1.19	1995	0.77	0.98	0.59	1.60
1981	0.49	0.77	0.48	1.23	1996	0.70	0.83	0.50	1.34
1982	0.64	0.85	0.53	1.35	1997	0.73	0.81	0.49	1.32
1983	0.51	0.82	0.52	1.31	1998	0.70	0.86	0.51	1.39
1984	0.59	0.99	0.62	1.57	1999	0.49	0.64	0.39	1.05
1985	0.89	1.35	0.84	2.14	2000	0.50	0.64	0.38	1.03
1986	0.74	1.20	0.75	1.91	2001	0.60	0.78	0.47	1.27
1987	0.70	1.30	0.81	2.06	2002	0.51	0.70	0.42	1.14
1988	0.86	1.56	0.98	2.48	2003	0.42	0.54	0.32	0.88
1989	0.58	1.10	0.69	1.75	2004	0.39	0.47	0.28	0.76
1990	0.66	1.18	0.74	1.88	2005	0.40	0.45	0.27	0.73
1991	0.50	0.95	0.59	1.51	2006	0.41	0.42	0.25	0.67
1992	0.92	1.16	0.72	1.85	2007	0.52	0.56	0.34	0.90
1993	1.06	1.16	0.72	1.85	2008	0.49	0.51	0.31	0.83
					2009	0.46	0.55	0.33	0.90
					2010	0.45	0.65	0.39	1.06
					2011	NA	0.69	0.37	1.26
					2012	0.79	0.73	0.43	1.21
					2013	0.61	0.51	0.30	0.84
					2014	0.34	0.41	0.25	0.68
					2015	0.62	0.80	0.48	1.32
					2016	0.72	0.70	0.42	1.15
					2017	0.88	0.85	0.51	1.39
					2018	0.56	0.54	0.32	0.89
					2019	0.44	0.65	0.38	1.07
					2020	0.40	0.62	0.36	1.04
					2021	0.37	0.65	0.38	1.10
					2022	0.58	0.74	0.42	1.28

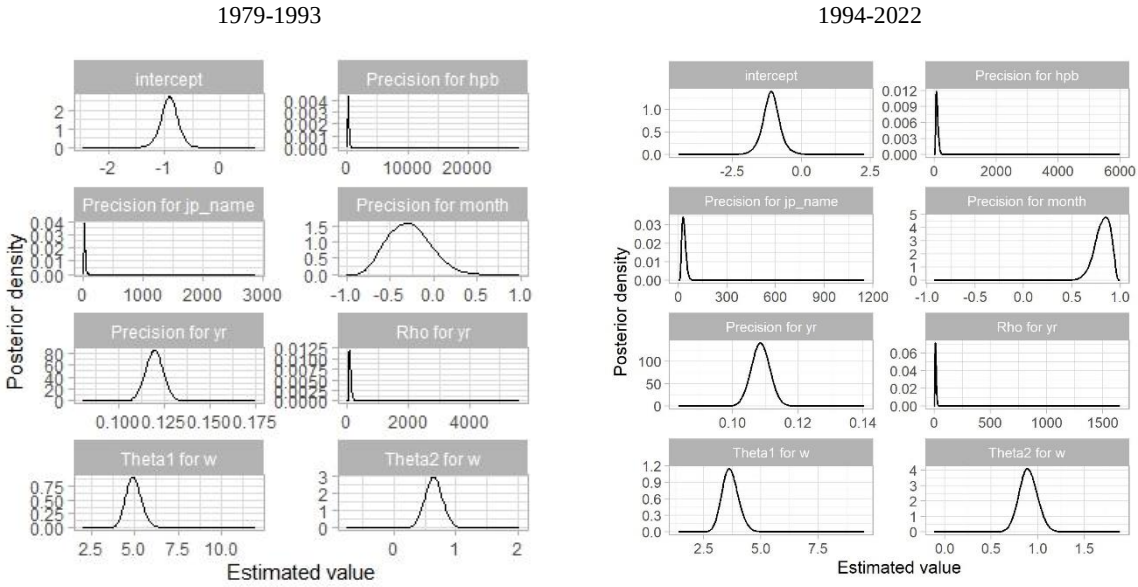

Fig. 13. Northeast. Posterior marginal distribution of the fixed effect (intercept), precision for random effects, temporal correlation term (Rho), and spatial field parameters (Thetas).

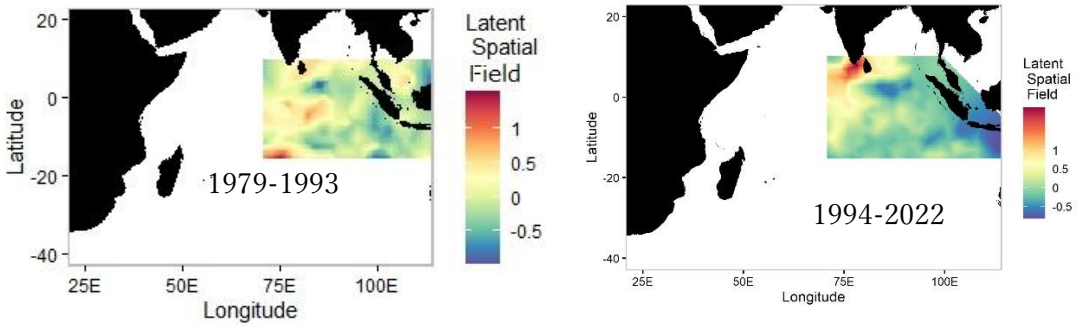

Fig. 14. Northeast. Mean of latent spatial field.

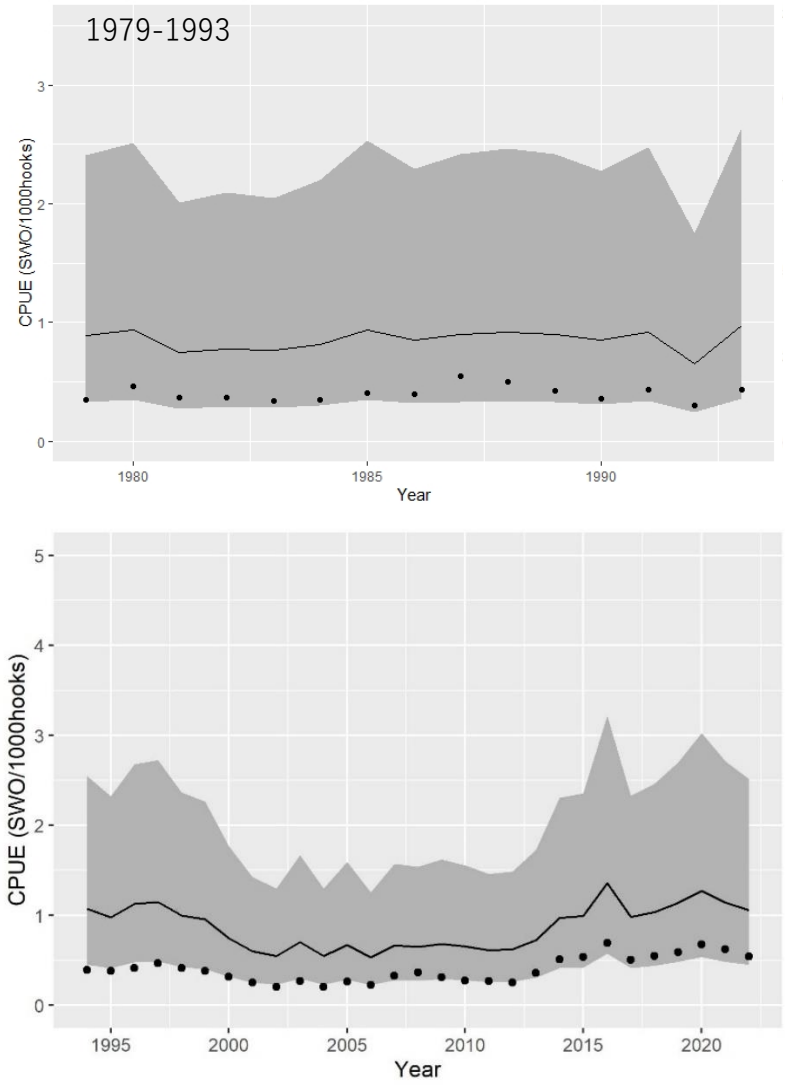

Fig. 15. Northeast. Historical changes of CPUEs. Line is standardized CPUE and filled area is 95% credible interval. Points denote nominal CPUE.

Table 3. **Northeast.** Nominal and standardized CPUEs for periods 1979-93 and 1994-2022.

year	nominal	Standardized	2.50%	97.50%	year	nominal	Standardized	2.50%	97.50%
1979	0.35	0.89	2.41	0.33	1994	0.39	1.07	0.45	2.55
1980	0.46	0.93	2.52	0.34	1995	0.38	0.98	0.41	2.32
1981	0.37	0.75	2.01	0.27	1996	0.42	1.13	0.48	2.68
1982	0.36	0.78	2.10	0.29	1997	0.47	1.15	0.49	2.73
1983	0.34	0.76	2.05	0.28	1998	0.42	1.00	0.42	2.36
1984	0.34	0.82	2.20	0.30	1999	0.38	0.95	0.40	2.26
1985	0.41	0.94	2.53	0.35	2000	0.32	0.75	0.32	1.77
1986	0.39	0.85	2.29	0.31	2001	0.25	0.60	0.25	1.43
1987	0.55	0.90	2.42	0.33	2002	0.21	0.55	0.23	1.30
1988	0.50	0.92	2.47	0.34	2003	0.27	0.70	0.30	1.67
1989	0.42	0.90	2.42	0.33	2004	0.20	0.55	0.23	1.30
1990	0.35	0.85	2.28	0.31	2005	0.26	0.67	0.28	1.59
1991	0.43	0.92	2.47	0.34	2006	0.23	0.53	0.22	1.26
1992	0.30	0.65	1.75	0.24	2007	0.33	0.66	0.28	1.57
1993	0.43	0.98	2.65	0.36	2008	0.36	0.65	0.27	1.54
					2009	0.31	0.68	0.29	1.62
					2010	0.28	0.65	0.28	1.55
					2011	0.27	0.61	0.26	1.46
					2012	0.25	0.62	0.26	1.48
					2013	0.36	0.73	0.31	1.73
					2014	0.51	0.97	0.41	2.31
					2015	0.54	0.99	0.42	2.36
					2016	0.69	1.36	0.57	3.22
					2017	0.50	0.98	0.41	2.33
					2018	0.69	1.04	0.44	2.46
					2019	0.69	1.14	0.48	2.70
					2020	0.69	1.27	0.54	3.02
					2021	0.69	1.14	0.48	2.71
					2022	0.54	1.06	0.45	2.52

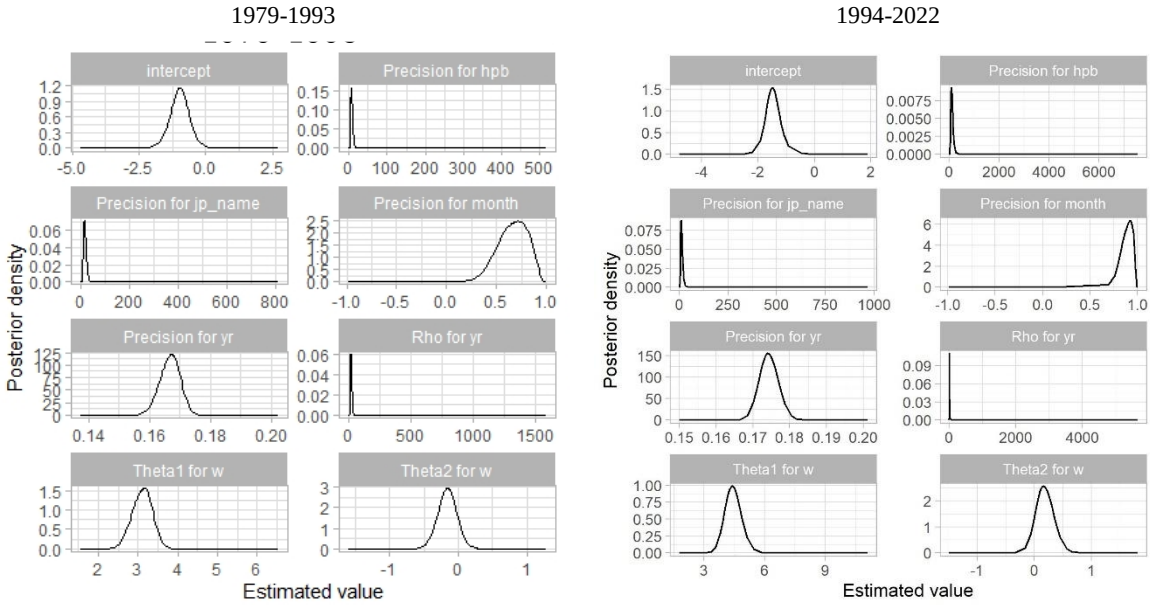

Fig. 16. Southwest. Posterior marginal distribution of the fixed (intercept), precision for random effects, temporal correlation term (Rho), and spatial field parameters (Thetas).

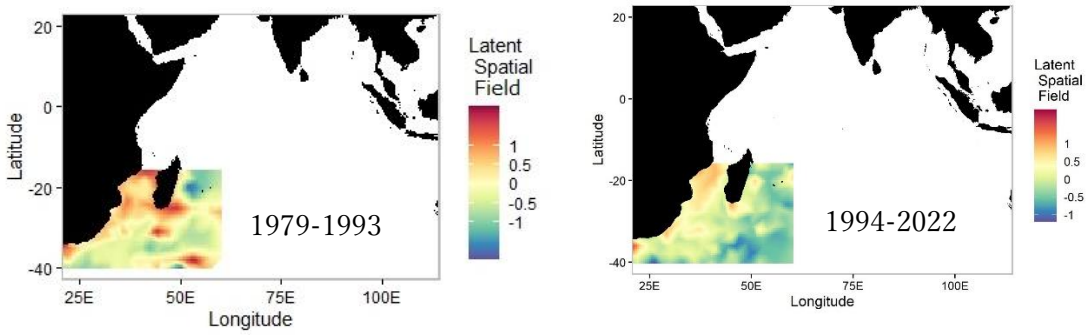

Fig. 17. Southwest. Mean of latent spatial field.

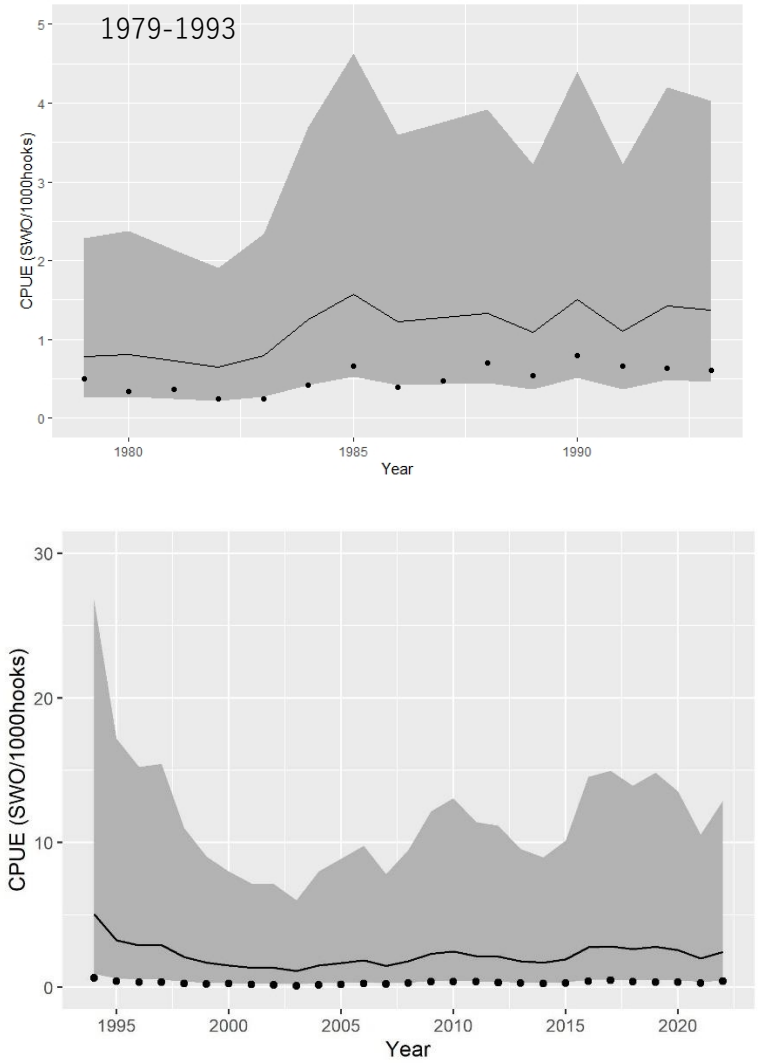

Fig. 18. Southwest. Historical changes of CPUEs. Line is standardized CPUE and filled area is 95% credible interval. Points denote nominal CPUE.

Table 4. **Southwest.** Nominal and standardized CPUEs for periods 1979-93 and 1994-2022.

year	nominal	Standardized	2.50%	97.50%	year	nominal	Standardized	2.50%	97.50%
1979	0.51	0.78	0.26	2.28	1994	0.66	5.07	0.95	26.72
1980	0.33	0.81	0.27	2.38	1995	0.42	3.26	0.61	17.20
1981	0.37	0.73	0.25	2.13	1996	0.35	2.89	0.54	15.23
1982	0.24	0.65	0.22	1.91	1997	0.37	2.93	0.55	15.46
1983	0.25	0.80	0.27	2.34	1998	0.27	2.09	0.39	11.00
1984	0.42	1.25	0.42	3.69	1999	0.23	1.72	0.32	9.05
1985	0.66	1.58	0.53	4.63	2000	0.26	1.52	0.28	8.00
1986	0.39	1.22	0.41	3.60	2001	0.19	1.36	0.25	7.18
1987	0.47	1.28	0.43	3.76	2002	0.16	1.35	0.25	7.14
1988	0.71	1.33	0.45	3.92	2003	0.12	1.14	0.21	6.01
1989	0.54	1.10	0.37	3.22	2004	0.17	1.52	0.28	8.03
1990	0.79	1.50	0.51	4.41	2005	0.21	1.68	0.31	8.88
1991	0.66	1.10	0.37	3.23	2006	0.26	1.86	0.35	9.79
1992	0.64	1.43	0.48	4.20	2007	0.23	1.48	0.28	7.82
1993	0.60	1.37	0.46	4.03	2008	0.30	1.80	0.34	9.51
					2009	0.39	2.31	0.43	12.16
					2010	0.37	2.48	0.46	13.07
					2011	0.37	2.17	0.41	11.44
					2012	0.32	2.12	0.40	11.16
					2013	0.28	1.81	0.34	9.55
					2014	0.26	1.70	0.32	8.98
					2015	0.29	1.92	0.36	10.14
					2016	0.43	2.76	0.52	14.54
					2017	0.47	2.84	0.53	14.96
					2018	0.38	2.64	0.49	13.93
					2019	0.36	2.82	0.53	14.86
					2020	0.36	2.57	0.48	13.56
					2021	0.29	2.00	0.37	10.56
					2022	0.43	2.44	0.46	12.91

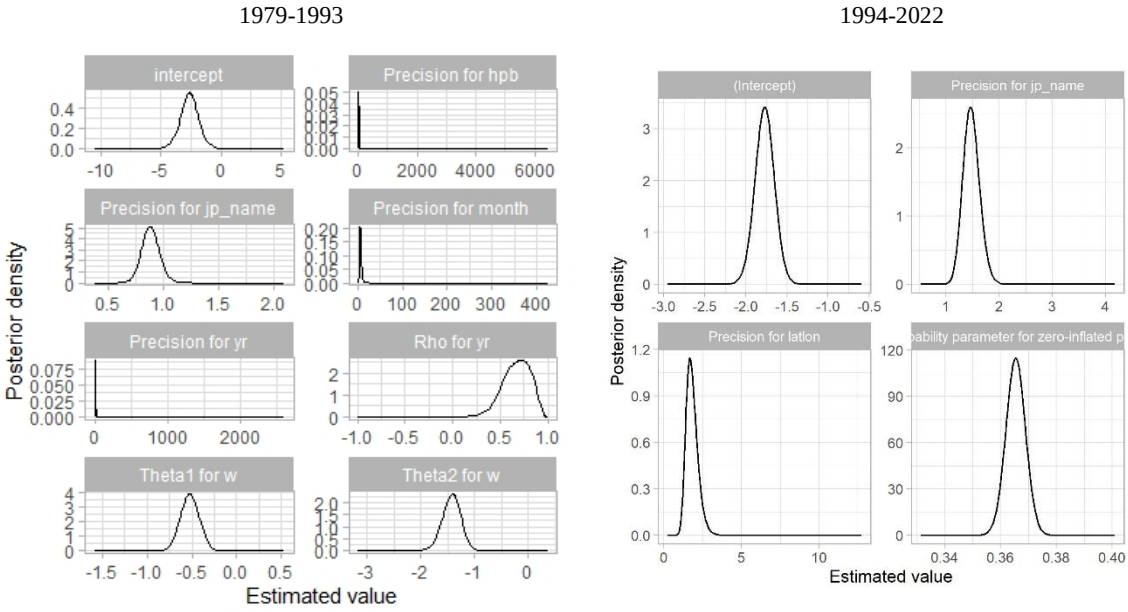

Fig. 19. Southeast. Posterior marginal distribution of the fixed (intercept), precision for random effects, temporal correlation term (Rho), and spatial field parameters (Thetas). Note no spatial model with no autoregressive (m_zip_glmm) during 1994-2022.

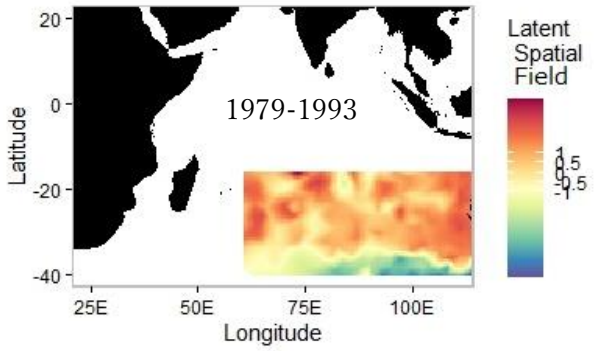

Fig. 20. Southeast. Mean of latent spatial field during 1979-1993. The lack of the figure during 1994-2022 is due to the non-spatial model (m_zip_glmm) during the period.

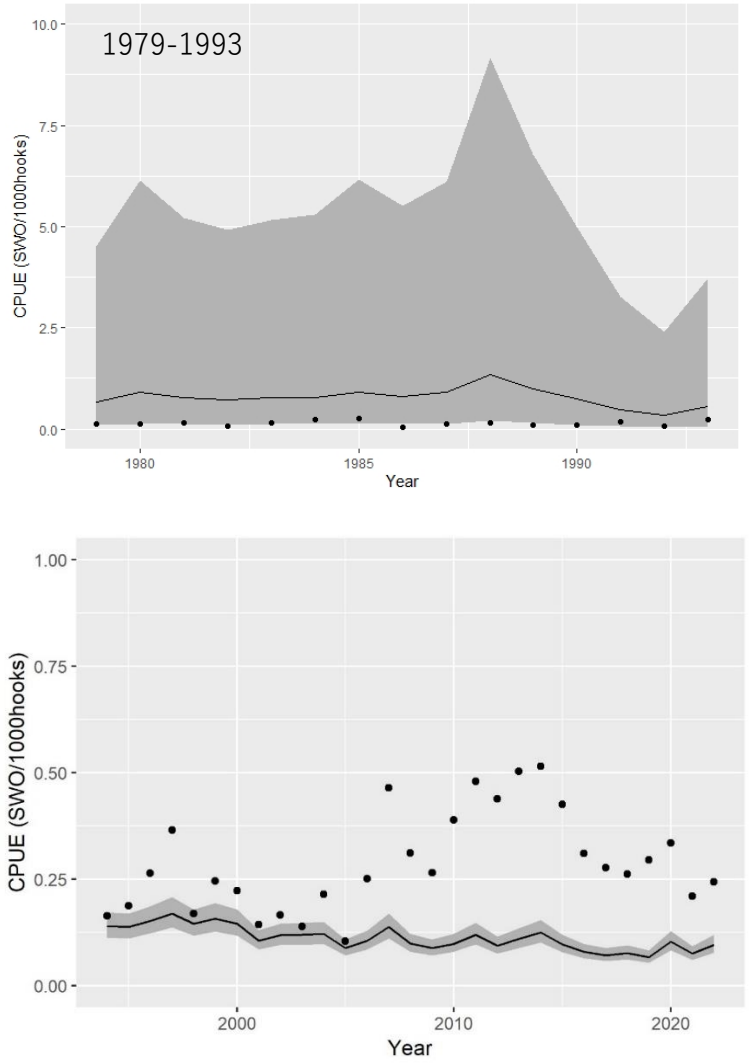

Fig. 21. Southeast. Historical changes of CPUEs. Line is standardized CPUE and filled area is 95% credible interval. Points denote nominal CPUE. Note the different scale of y axis for CPUE between the periods.

Table 5. **Southeast.** Nominal and standardized CPUEs for periods 1979-93 and 1994-2022.

year	nominal	Standardized	2.50%	97.50%	year	nominal	Standardized	2.50%	97.50%
1979	0.12	0.66	4.52	0.10	1994	0.16	0.14	0.11	0.17
1980	0.13	0.90	6.14	0.13	1995	0.19	0.14	0.11	0.17
1981	0.15	0.77	5.21	0.11	1996	0.26	0.15	0.12	0.19
1982	0.08	0.72	4.91	0.10	1997	0.37	0.17	0.14	0.21
1983	0.14	0.76	5.16	0.11	1998	0.17	0.15	0.12	0.18
1984	0.22	0.78	5.28	0.11	1999	0.25	0.16	0.13	0.19
1985	0.26	0.90	6.15	0.13	2000	0.22	0.15	0.12	0.18
1986	0.05	0.81	5.51	0.12	2001	0.14	0.11	0.09	0.13
1987	0.12	0.90	6.11	0.13	2002	0.17	0.12	0.10	0.15
1988	0.14	1.35	9.16	0.20	2003	0.14	0.12	0.10	0.15
1989	0.10	1.00	6.78	0.14	2004	0.21	0.12	0.10	0.15
1990	0.11	0.74	5.01	0.11	2005	0.11	0.09	0.07	0.11
1991	0.18	0.48	3.27	0.07	2006	0.25	0.11	0.09	0.13
1992	0.08	0.35	2.40	0.05	2007	0.46	0.14	0.11	0.17
1993	0.22	0.54	3.72	0.08	2008	0.31	0.10	0.08	0.12
					2009	0.27	0.09	0.07	0.11
					2010	0.39	0.10	0.08	0.12
					2011	0.48	0.12	0.10	0.15
					2012	0.44	0.09	0.08	0.12
					2013	0.50	0.11	0.09	0.14
					2014	0.52	0.13	0.10	0.15
					2015	0.43	0.10	0.08	0.12
					2016	0.31	0.08	0.06	0.10
					2017	0.28	0.07	0.06	0.09
					2018	0.26	0.08	0.06	0.10
					2019	0.30	0.07	0.05	0.08
					2020	0.34	0.10	0.08	0.13
					2021	0.21	0.08	0.06	0.09
					2022	0.24	0.10	0.08	0.12

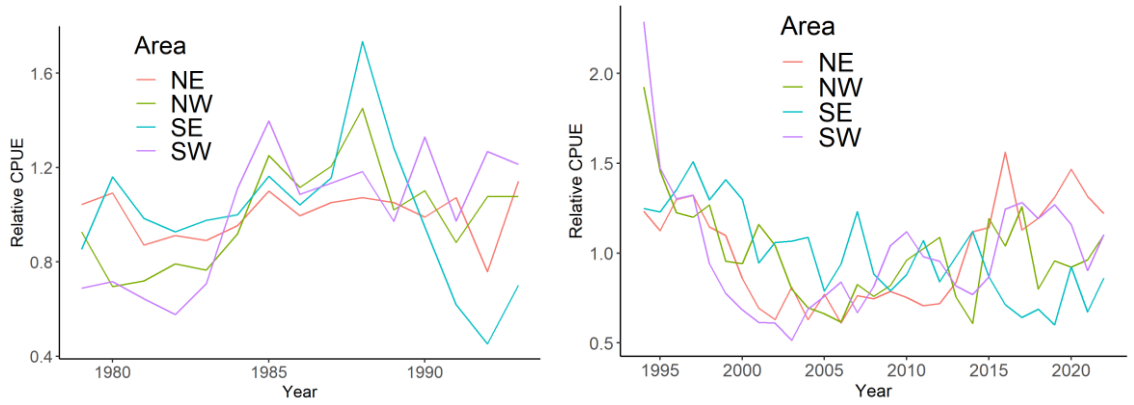

Fig. 22. Comparison of relative standardized CPUE of swordfish caught by Japanese longline fisheries for the four areas in the Indian Ocean.

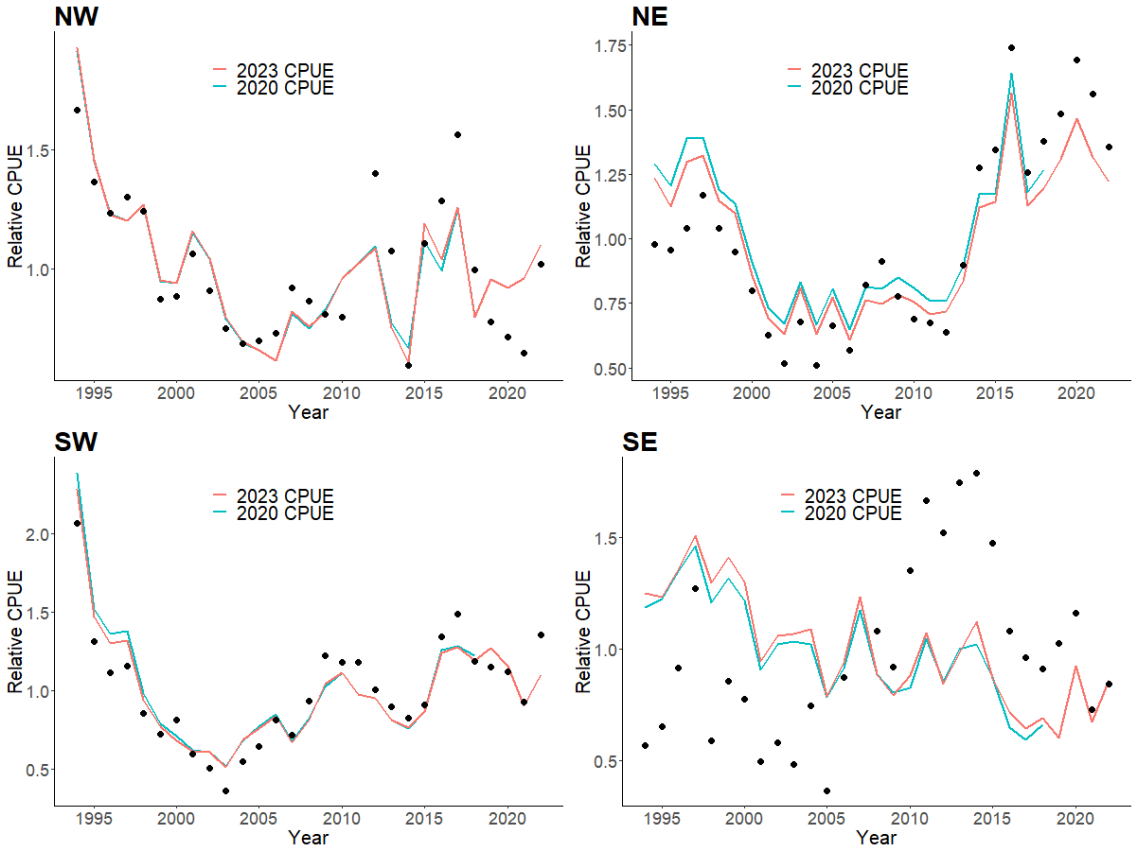

Fig. 23. Comparison of relative standardized CPUE of swordfish for the four areas in the Indian Ocean by Japanese longline fisheries during 1994-2022 from this study (blue solid lines) and Taki et al. (2020) (red solid lines). Black circles show nominal CPUE.